ARCH SOC ESP OFTALMOL 2006; 81: 527-536 **ORIGINAL ARTICLE**

TRABECULOPLASTY WITH TWO DIFFERENT LASERS IN CATS, MONKEYS AND HUMANS: A SCANNING ELECTRON MICROSCOPY STUDY

TRABECULOPLASTIA CON DOS TIPOS DE LÁSER EN GATO, MONOS Y HUMANO: ESTUDIO MORFOLÓGICO CON MICROSCOPÍA ELECTRÓNICA DE BARRIDO

SIMÓN G[1]

ABSTRACT

Purpose: To study the structural changes induced by trabeculoplasty with two different lasers (Ti-Sph and argon) and observe the differences between four trabecular meshwork models.
Materials and methods: Four different trabecular meshwork (TM) models were used from cats, monkeys, and humans. This study was performed on fresh cadaver eyes («ex vivo») except for the cat in which this study was performed «in vivo». The morphology of the trabecular meshwork was observed by scanning electron microscope (40/100X) after being treated with argon (0.1s/pulse, 600 to 1,000mW, 50µ spot size) and Ti-Sph (7µsg/pulse, 25 to 110mJ,175µm of spot size). The study on cats allowed assessment of the induced effect after 24 hours, and 4 weeks after the treatment on the TM. Typical clinical trabeculoplasty parameters were used for both lasers during this study.
Results: The models used in this study were found to be adequate for trabeculoplasty. They exhibited a deep anterior chamber and an accessible TM. The argon laser induced significant changes in the TM in all models studied. The cat model demonstrated

RESUMEN

Objetivo: Verificar el impacto estructural inducido por la trabeculoplastia con dos tipos de láser, Titanio-Zafiro (Ti-Za) y argón sobre cuatro tipos de malla trabecular.
Material y Métodos: Se utilizaron cuatro tipos diferentes de malla trabecular procedentes del gato doméstico, dos tipos de monos y humano. Este estudio se practicó sobre ojos frescos de cadáver («ex vivo»), excepto en el gato, en el que se realizó «in vivo». La morfología observada bajo un microscopio electrónico de barrido (40/100X), se efectuó sobre las mallas trabeculares tratadas con argón a 0,1 sg/pulso, de 600 a 1.000 mW, y 50 mm de diámetro de spot y para el Ti-Za, a 7 msg/pulso, de 25 a 110 mJ y 175 mm de diámetro por spot. El estudio en gato permitió analizar el efecto inducido a las 24 horas y 4 semanas después del tratamiento. Los parámetros utilizados comprenden los rangos de la trabeculoplastia clínica para ambos láseres.
Resultados: Los modelos utilizados fueron muy adecuados para la práctica de la trabeculoplastia, observando una cámara profunda y un ángulo muy accesible a la acción del láser. El láser de argón fue

Received: 22/9/05. Accepted: 21/9/06.
Boston University, Biomedical Engineering Dept. Boston, Massachussets, United States.
[1] Ph.D. in Medicine.

Correspondence:
Gabriel Simón
Instituto Oftalmológico Gabriel Simón
C/ Fuencarral, 7
28007 Madrid
Spain
E-mail: gabrielsimon@dr-simon.net

TM repair response one month after treatment. For Ti-Sph, high levels of energy (>100mJ) were required to induce significant structural changes in the TM.
Conclusion: The IOP reduction effect by argon trabeculoplasty (600/1,000mW) induced structural shrinkage of the collagen in the TM via thermal effects. The Ti-Sph laser works through non-structural mechanisms. At clinical levels (lower than 80mJ), Ti-Sph does not show evidence of TM changes *(Arch Soc Esp Oftalmol 2006; 81: 527-536).*

Key words: Scanning electron microscopy, trabeculoplasty, Ti-Sapphire, argon, trabecular meshwork.

el que provocó una mayor alteración del tejido trabecular en todos los modelos. La malla trabecular del gato demostró capacidad de reparación después de un mes del tratamiento. Para el Ti-Za fue necesario el uso de energías superiores a los 100 mJ para inducir un cambio estructural evidenciable en la malla trabecular a 100X.
Conclusiones: El efecto de la trabeculoplastia con argón (600/1.000 mW) sobre la malla trabecular implica una alteración «estructural» producida por la contracción del colágeno en el punto tratado (efecto térmico). Para el láser de Ti-Za y a niveles energéticos inferiores a 80mJ no se produce ningún cambio estructural.

Palabras clave: Microscopía electrónica de barrido, trabeculoplastia, Titanio Zafiro, argón, malla trabecular.

INTRODUCTION

Traditionally, two drainage routes for aqueous humor have been described for different species: the trabecular or conventional route, which channels the aqueous fluid from the anterior chamber to the episcleral veins via the trabecular meshwork; the uveo-scleral or non-conventional route (1,2) which eliminates aqueous flow via the ciliary meshwork up to the suprachoroidal space. This last draining route is very active during the first third of life, becoming more passive in time until amounting to barely 10% of total drainage value in human adults (3,4). The trabecular meshwork is easily accessed by laser using a gonioscopic lens, which facilitates acting upon it in order to reduce opposition to fluid (5) (trabeculoplasty). This bloodless method is used by outpatient care services. Trabeculoplasty with argon laser has proven to be effective in the treatment of glaucoma (6,7), generally known to act through thermal and biological effects. During clinical applications, it is possible to notice a whitening of the spot treated (50 mm) and a retraction of neighboring tissues. The rise of hypertensive peaks after surgery has also been described in relation to the chosen energy magnitude; in a small number of cases (3%) (8) there has been an increase in intraocular pressure in the long run. This kind of trabeculoplasty is limited to a number of impacts, since coagulated spots on the trabecular meshwork are not functionally active. The need for laser seems contradictory, since it destroys a particular area of the trabecular meshwork, despite the fact that its purpose is to induce a greater permeability in the untreated trabecular meshwork.

Recently, the use of a new laser with a 790 nm wavelength and 7 µsg exposure pulses has been introduced to perform clinical trabeculoplasty.

This type of laser is not thermal, and its action is not presently defined. This wavelength was used in pilot studies using conventional trabeculoplasty methods (9), which could have greater hypotensor effects and entail the possibility of applying them regularly and reducing damage to local tissues.

SUBJECTS, MATERIAL AND METHODOLOGY

Four different models were used for the trabecular meshwork, three *ex vivo*: Cynomolgus (*Macaca fascicularis*), Rhesus (*Macaca mulatta*), human and one *in vivo* in cats (*Felis domesticus*). The four models show similar anatomical traits for aqueous trabecular drainage (conventional route). The three *ex vivo* models belonged to very closely related species, and the eye's structure exhibited minimal differences. In all cases, curvature, energy and corneal thickness was normal, and the chamber's dimensions and exposure of the trabecular meshwork were optimal.

In vivo Model

Research protocols used for cats were obtained after approval by the animal research committee at Miami University. Handling of animals was performed in compliance with ARVO's resolution regarding the treatment of laboratory animals for research purposes. Two groups (A and B) were used consisting of six 1-year-old female domestic cats (n=12) and they were monocularly treated with two lasers. All underwent full ophthalmic examination before treatment with previously calibrated argon laser (514 nm, .1 s/pulse, 600 to 1,000 mW, 50 m spot diameter) and Ti-Za laser (Ti: Al2O3, 790 nm, 7 µs/pulse, de 25 to 110mJDE3, 175 µ spot diameter). All animals were treated under general anesthesia (ketamine hydrochloride, 20 mg/kg of weight, 1 mg/kg of acepromazine maleate, and 0.20 mg/kg of atropine sulfate) using a device specially designed to facilitate handling. The lasers used were commercially available (argon by Coherent Inc, Palo Alto, USA and Ti-Za by Solx C. Boston, USA), and were applied using a pediatric gonioscopic lens. The scope of the angle treated was 180º. The number of impacts ranged from 40 to 60; in no case were they confluent, set apart at a distance which was double the spot's size (250 µm or every 3.6º). The impact was located on the trabecular meshwork, between the Schwalve line and the scleral spur. In all cases the tissues reacted to the application of laser in a similar way to that observed in humans, i.e. whitening, bubbles (fig. 1) and induction of cellular or inflammatory tyndall. Twenty-four (24) hours later, it was already difficult to appreciate the initial whitening; 14 days later it was impossible (fig. 1). In two cases, a small break in the vascular network of the treated area was observed, leading to a slight transitional hematic tyndall without hyphema. No topical miotic drugs were used during treatment. During the period following surgery, no evidence was found of ocular nor general alterations. Twenty-four (24) hours after treatment, six eyes were processed, three from the group treated with Ti-Za and three with argon, to be studied under electronic microscopy, while the rest were processed 4 weeks later.

Ex vivo Model

Two pairs of eyes were taken from the laboratory for studies in primates at Miami University (a 6-year-old rhesus monkey and a 12-year-old Cynomolgus monkey), plus one pair of fresh eyes belon-

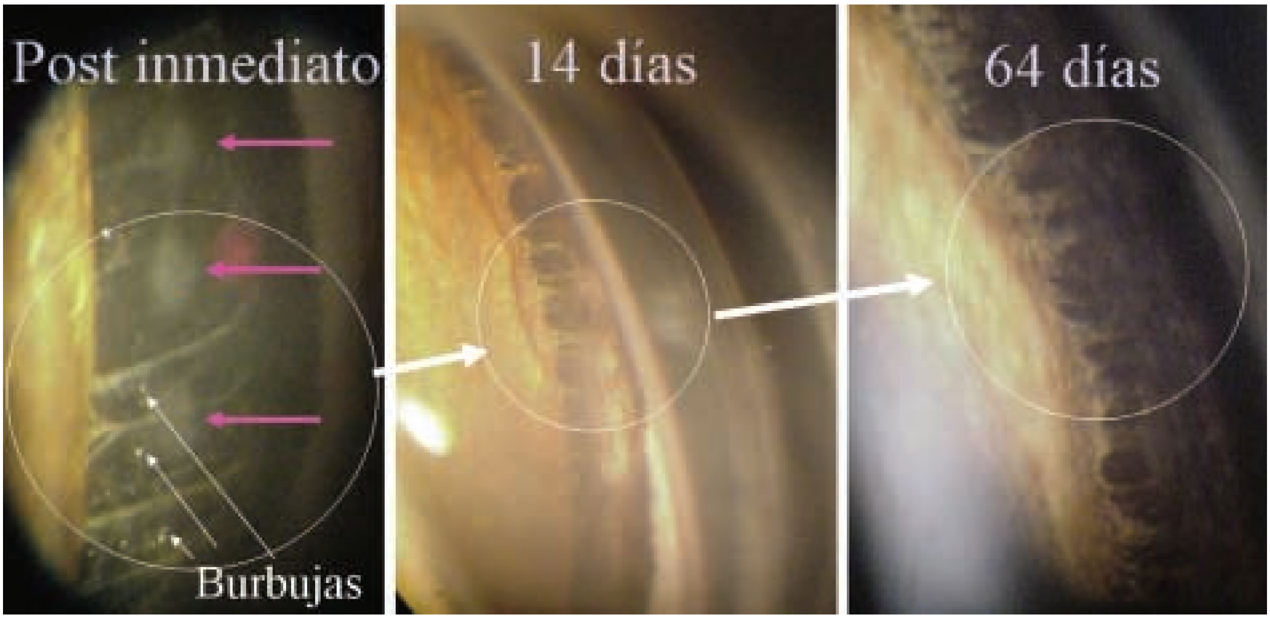

Fig. 1: Spot treated with TiZa laser. Initial image after 14 days and 2 months, respectively.

ging to the Florida Lyons Eye Bank (a human male aged 69). All showed one obitus less than 12 hours without exhibiting any eye alterations nor past surgical procedures under biomicroscopic exam. Since the same eye was used to perform trabeculoplasties both with argon and Ti-Za, and in order to prevent any factor that may affect the rate of absorption of laser energy through the cornea and aqueous humor (corpse eyes), the procedure went as follows (fig. 2): six equidistant marks were drawn on the limbo-corneal with a blue methylene marker to divide the cornea's perimeter into six identical fragments. Subsequently, each sector previously marked off along the limbo was dissected using a diamond knife (60º each) in order to divide the section corresponding to the iris and eliminating the lens for better angle exposure (fig. 2C). Between each mark, six 10-0 nylon stitches were placed in order to identify the spot to be treated with laser and thus facilitating its identification after fixing and processing it with a scanning electron microscopy. Each eye was treated with both laser techniques and three different energy levels (one treatment per section). The following energies were used with argon laser: 600, 800 and 1000 mW for all eyes, and with Ti-Za laser: 15, 30, 50mJ for three eyes and 80, 100 and 130mJ for the remaining three (SD 3mJ). Treatment was thus performed through the air and straight into the trabecular meshwork (between the Schwalve line and the scleral spur) without resorting to a gonioscopic lens (fig. 2C, D).

After treatment was completed, each eye section was processed in order to be analyzed under scanning electron microscopy.

Prior to that, they were fixed in 2% paraformaldehyde and 2.5% glutaraldehyde and then in 1% osmium tetroxide for two hours in series of critical-point ethanol dehydration (carbon dioxide). They were then saturated with gold (Hummer V, Technics, Alexandria, USA) and examined under electronic microscope (JSM-35, JEOL Ltd., Tokyo, Japan) with 25 kV acceleration voltage.

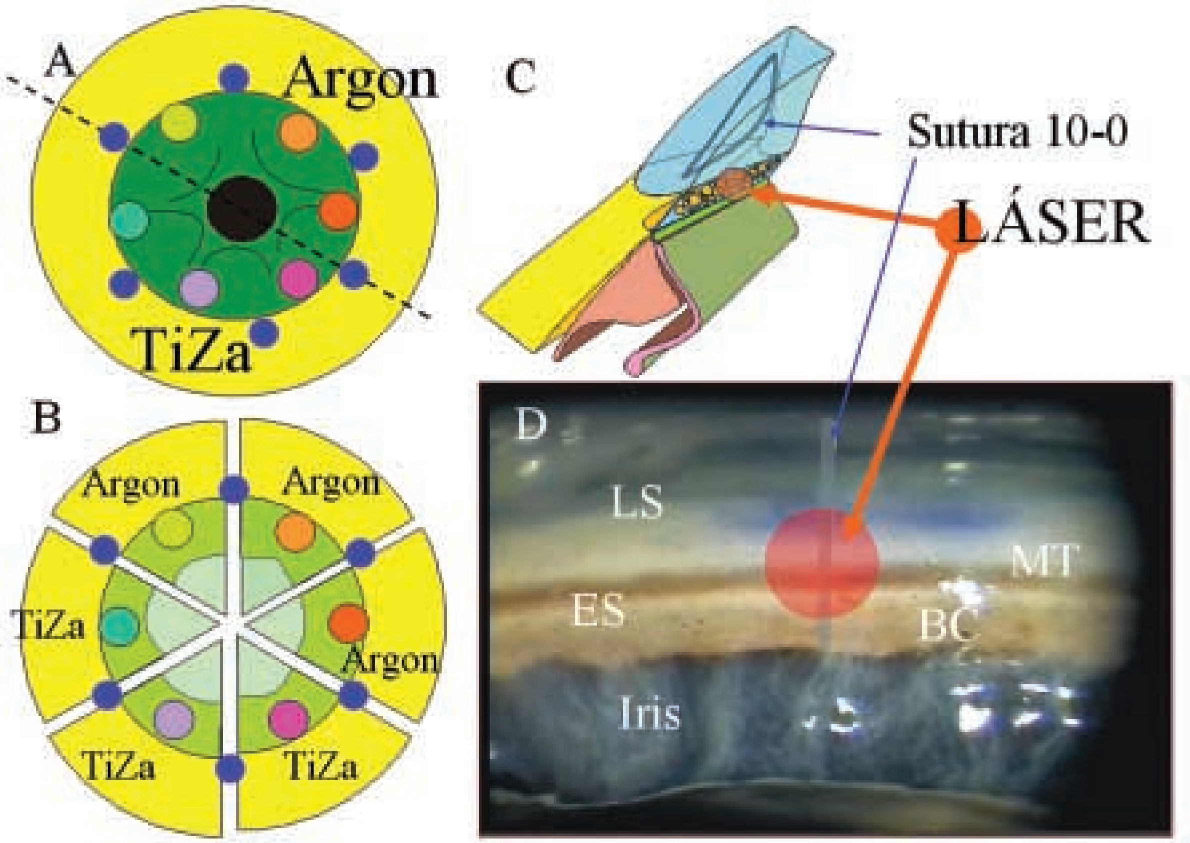

Fig. 2: Globe preparation before an ex vivo trabeculoplasty. LS (Schwalbe Line), MT (Trabecular Meshwork), ES (Scleral Spur), BC (Ciliary Band).

FINDINGS

In Vivo Model

Figure 3 shows a photographic composite of one sector (around 45º) in the trabecular meshwork treated with laser for the purpose of the present study. The image corresponds to a domestic cat's eye treated one month earlier with 12 Ti-Za laser impacts. The exposed trabecular meshwork does not show any alterations or signs revealing the location where the laser made impact. Energy level used was 50 mJ, identical to that proposed for trabeculoplasty in humans. In the image, twelve circles signal the spots hit by laser. The size of the circle corresponds to the relative dimensions of the spot (175 µ), distance between impact points (250 µ) and size of the cat's trabecular meshwork. Obviously, the place taken up by the circle on the trabecular meshwork in the image does not necessarily correspond to the exact location of treatment. Figure 4 shows the sequences corresponding to the study of the domestic cat one day and one month after treatment. Column B shows control images of an untouched trabecular meshwork. Column A shows treatment with argon. Columns C, D and E show tissue reaction to three different energy levels using Ti-Za laser. The upper section corresponds to the study performed immediately after treatment, and the lower section to that one month later. There is a significant destructuring of the trabecular meshwork after argon treatment 24 hours and one month later, when tissue repair had consolidated.

Meshworks treated with Ti-Za revealed no alterations when applying energy levels lower than 81mJ (columns C and D). Segments receiving more than 100mJ were barely broken along the filaments making up the trabecular meshwork when analyzed 24 hours after treatment, exhibiting no changes one month later (fig. 4E).

Ex Vivo Model

Observations regarding the Cynomolgus and Rhesus models were similar (figs. 5 and 6). The

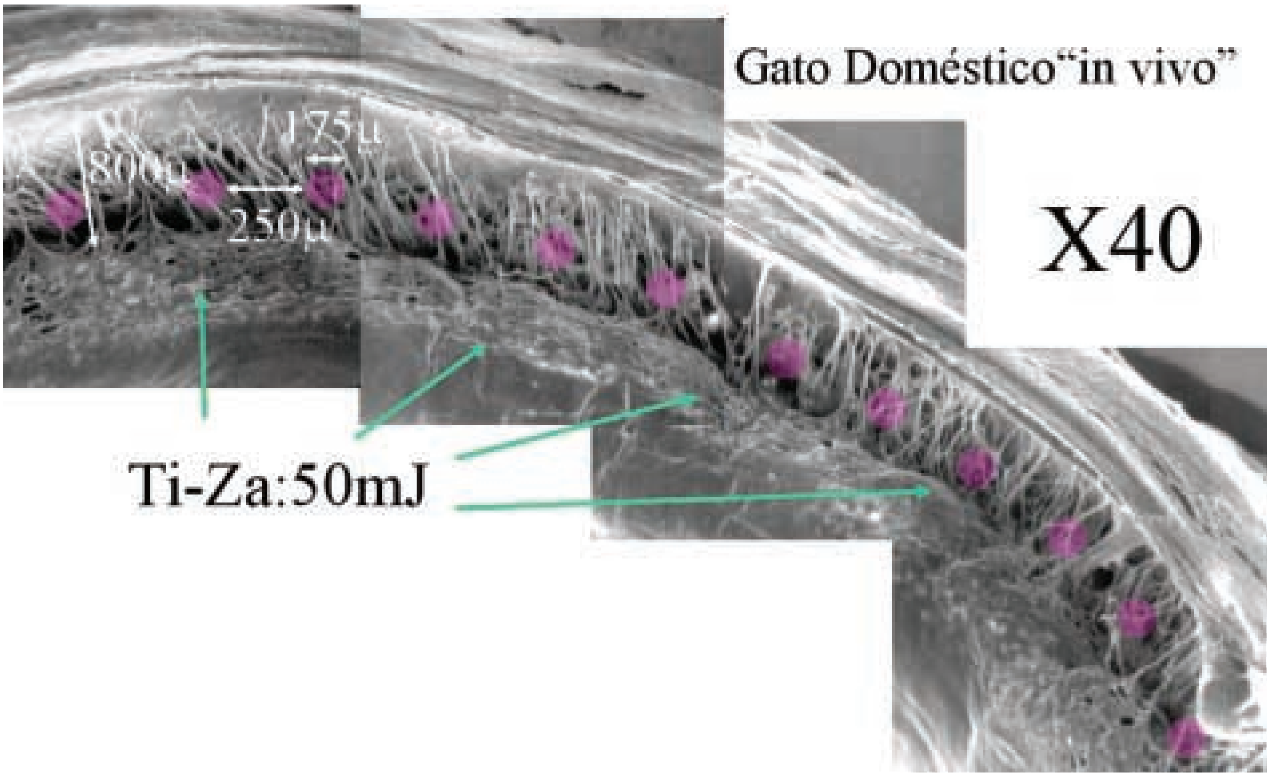

Fig. 3: Angle section of the cat treated with Ti-Za laser (50 mJ). This energy level corresponds to the one used in clinical trabeculoplasty. One month later, no alterations on the trabecular meshwork were appreciated in the exposed area.

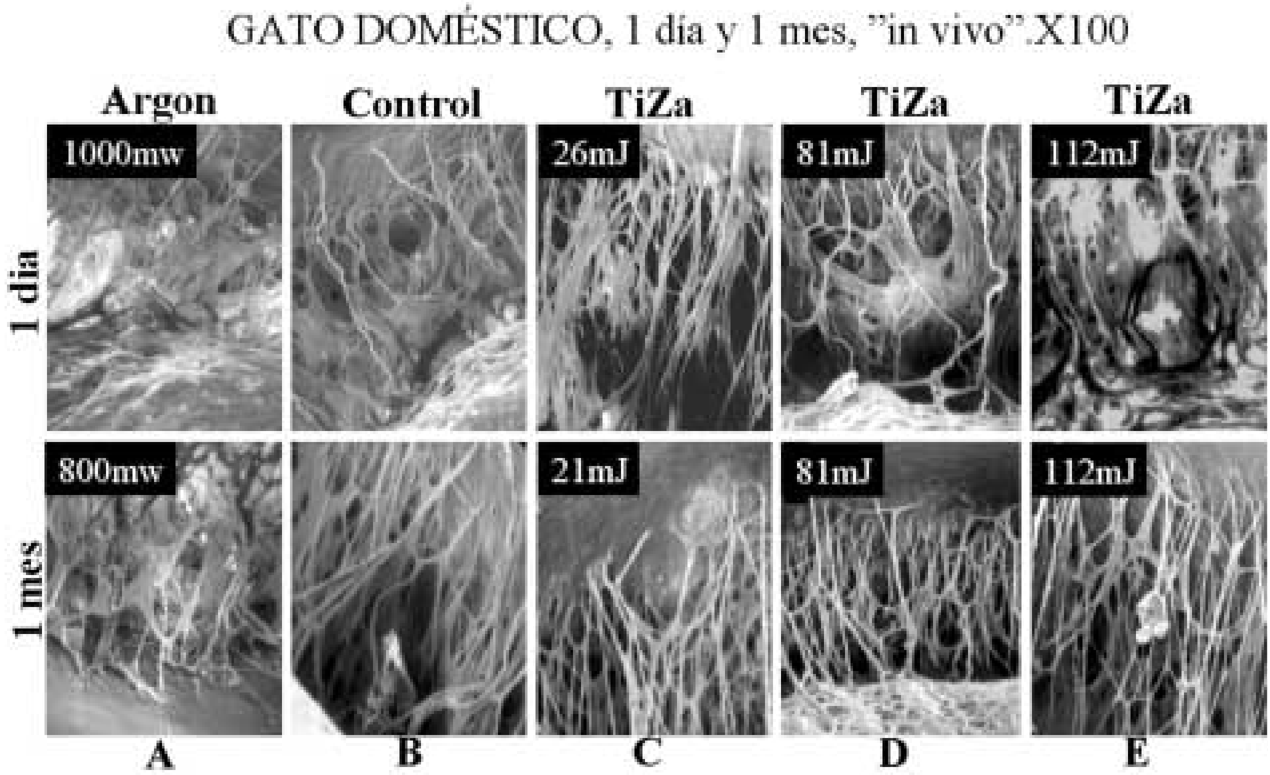

Fig. 4: Structural change was apparent immediately after argon and Ti-Za laser were applied, and seemed to be repaired one month later.

control image revealed a trabecular architecture which was almost identical in terms of dimension and structural disposition. The argon laser impact (A) caused clear destructuring of the trabecular meshwork in a crater-like shape and translated into radial folds caused by collagen-induced compression partially spurred by laser thermal effects. The Cynomolgus monkey's image showed two spots hit by laser on the trabecular meshwork tangential to the Schwalbe line on a 100X image (fig. 5A). Under the Rhesus monkey model, using Ti-Za laser and energy levels below 50mJ no significant effect was observed on the trabecular meshwork (fig. 6C, D). As for the Cynomolgus monkey, some alterations were noticed when applying energy levels exceeding 80 mJ in 30% of the impact points (fig. 5D) and in both monkeys, Rhesus and Cynomolgus, leaks on the trabecular meshworks were observed when using energy levels above 110 mJ (C). Images obtained for the human model showed a more delicate and well-defined trabecular meshwork than that of the previous two models, although similar in dimensions and structure. Argon trabeculoplasty (fig. 7A) showed a compact, smooth area where no trabecular architecture was appreciated.

The surrounding tissue quickly recovered its control aspect. No alterations were observed either when using energy levels below 50 mJ with Ti-Za laser, although there were cases of broken plaques belonging to the first layers of trabecular meshwork, letting see through the underlying tissue (7D). When applying 100 mJ energy levels, a very deep alteration was observed around Schlemm's canal (7E). 130 mJ energy level was capable of generating a marked tissue dehiscence (7F), and in some cases even deinsertion of the iris root.

DISCUSSION

Although the active principle in argon laser trabeculoplasties remains controversial, it is possible to observe the mechanical traction effect induced on the trabecular meshwork surrounding the coagula-

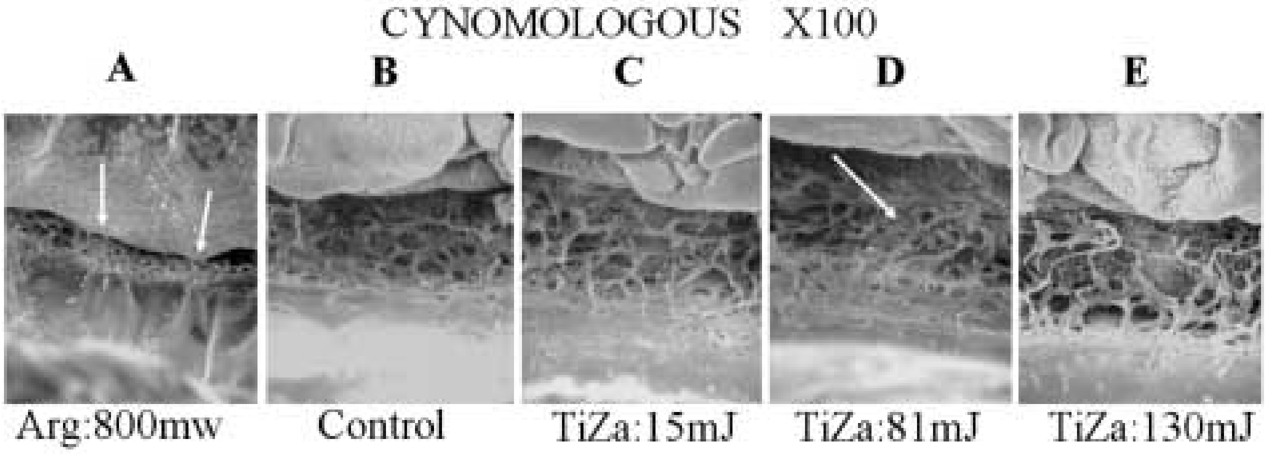

Fig. 5: No variations were observed on the trabecular meshwork (C) until 81 mJ energy level was applied (D). At 130 mJ, a sizeable alteration of the trabecular meshwork architecture took place (E). Argon impacts (A) revealed the contraction suffered by local collagen.

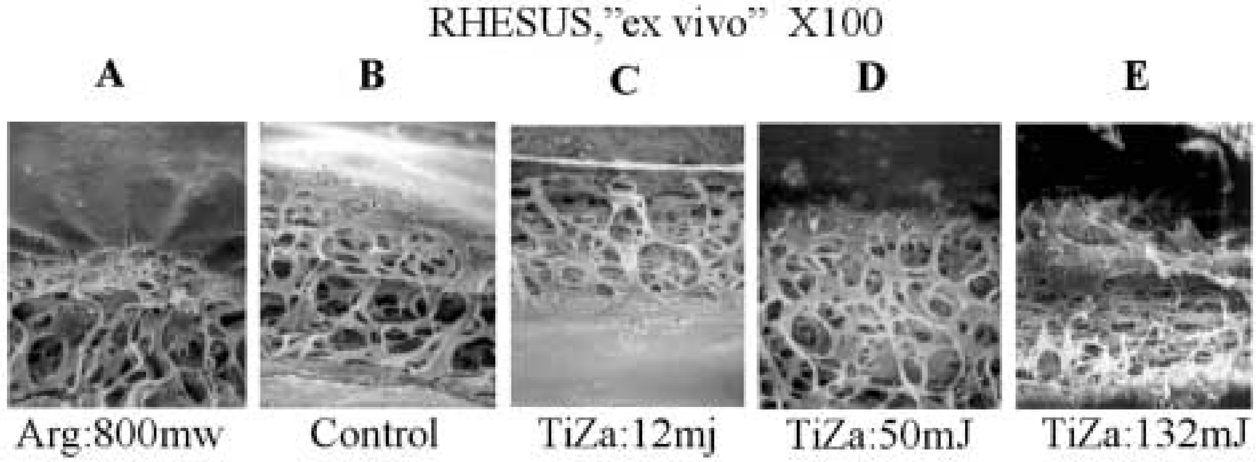

Fig. 6: No structural changes were observed at 12 y 50 mJ using Ti-Za (C,D). Image A clearly showed the point of absorption for thermal energy delivered by argon laser. A crater of tissue destruction and radial contraction lines were detected (A).

ted spots caused by collagen aggregation. This phenomenon could be compared to the one achieved on the cornea when performing photothermal ketaroplasty (11). Several authors have analyzed the impact of argon laser on the trabecular meshwork alluding to this biomechanical effect (12-14).

The suggested spot where laser impacts should focus on the intersection between the pigmented and non-pigmented trabecular meshwork. It would seem contradictory to eliminate a specific area within the trabecular meshwork in order to achieve a greater permeability for the trabecular tissue found between two impacts (15). Usually, thermal trabeculoplasties use 50 and 60 impacts distributed along two sessions, spot size ranging between 50 and 100 µ. This 360º distributed impact density suggests that application should be made every 3.6º (16) (360/100). In humans, the area covered by the trabecular meshwork resembled that of a 300-400µ-wide circular band with a 6 mm radius. The estimated area yielded a value of 11.3 mm^2 (300 x 2 πr). The estimated area treated with laser was approximately 0.25 mm^2 (120 impacts x π 252 m), i.e. this type of trabeculoplasty destroys at least 2% of its

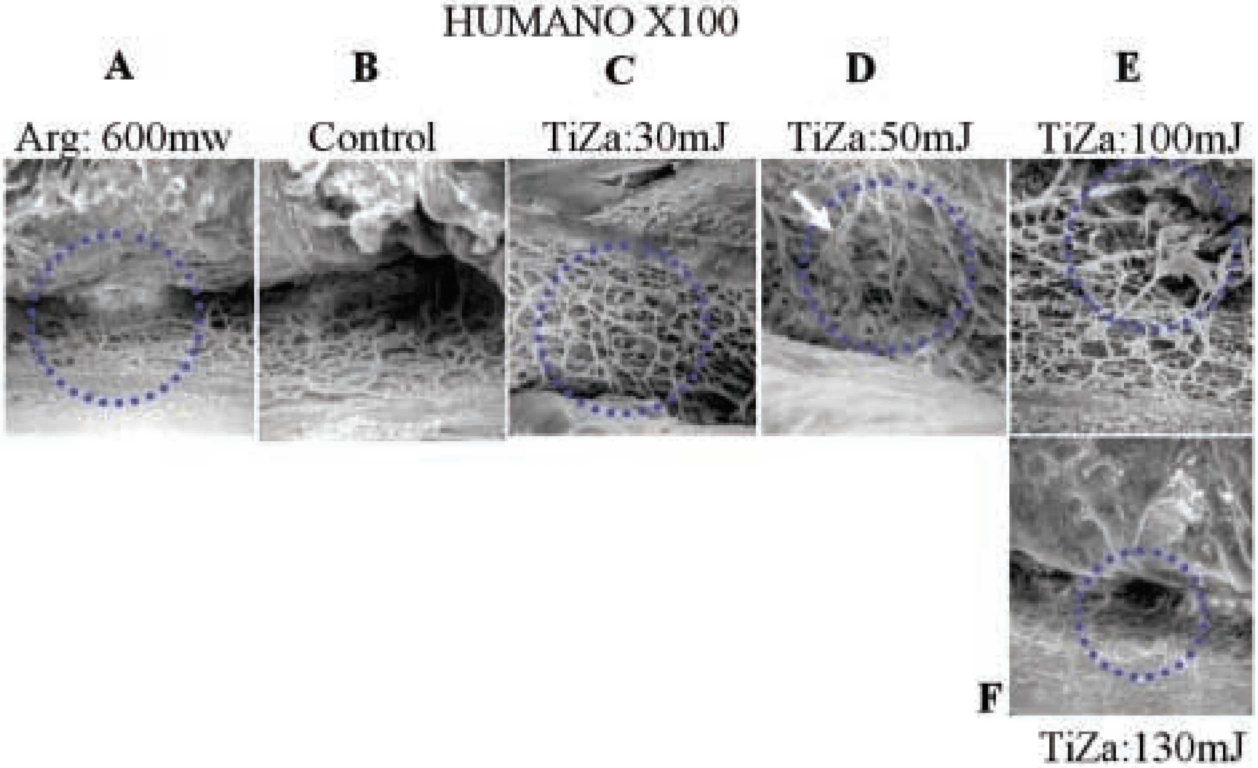

Fig. 7: The thermal effect is less obvious here than in the remaining models (A). TiZa clinical energy levels did not cause alterations on the trabecular network (C,D,E) until they reached values well above those used in trabeculoplasties.

trabecular meshwork. After a 5-year follow-up and one trabeculoplasty with argon, at least 50% of all cases exhibited inadequate IOPs. Re-treatment with argon has been shown to be scarcely effective and is associated with high failure rates (17,18).

The use of cold laser mitigates the damage suffered by the trabecular meshwork, and in theory it should be feasible to perform regular trabeculoplasties to improve the trabecular route. The active principle for this type of wavelength (790 nm) will be controversial, and possibly hard to solve for good. One theoretical model (10) was proposed capable of predicting the high penetration of Ti-Za laser across the trabecular meshwork. It is likely that the greater penetration of wavelengths amounting to approximately 800 nm may explain the greater efficacy in reducing IOP (10). The spot size caused by Ti-Za laser (175 µ) is greater than that of argon (50 µ); subsequently, a trabecular meshwork treatment consisting of 50 impacts would represent a 1.5 mm^2 area or 10% of the total filtering area. Micrographies of the trabecular meshwork treated with energy levels below 100 mJ barely show any alterations (figs. 4, 5, 6 and 7), and the energy level recommended for clinical trabeculoplasty is even lower, between 20 and 50 mJ (fig. 3). Of all the models introduced herein, only the domestic cat was treated *in vivo* and under the same clinical conditions as humans (gonioscopic lens). The remaining models were subjected *ex vivo* to laser through the air instead of going through the cornea and aqueous fluid, so that the amount of energy reaching the trabecular meshwork is slightly higher (approximately 15% more). Stoiber et al (19) point at an active principle associated with the absorption of laser energy by intracellular and interstitial melanine on the trabecular meshwork (ablation phenomenon). This fact could eliminate a certain amount of trabecular melanine and decrease its opposition to inflow of aqueous humor. It is also likely that the shock wave generated by this process induces a local inflammatory response by attracting phagocytic cells that also eliminate tissue detritus and amorphous extracellular material. These facts are consistent with the absence of damage observed on the trabecular meshwork at the structural level after being treated with Ti-Za laser, supporting the prescription of regular trabeculoplasty with this type of laser to treat glaucoma.

Although no morphological changes were found on the trabecular meshwork after using Ti-Za laser in 40/100X magnification, it is feasible that such changes take place at a lower structural level. Laser interaction with the trabecular meshwork could trigger a chain of events difficult to list (both biological and/or biochemical) which determine a smaller opposition to aqueous inflow through the meshwork, from the anterior chamber up to Schlemm's canal.

REFERENCES

1. *Bill A. The aqueous humor drainage mechanism in the cynomolgus monkey (Macaca irus) with evidence for unconventional routes. Invest Ophthalmol 1965; 4: 911-919.*
2. *Bill A. Phillips CL. Uveoscleral drainage of acuose humor on human eyes. Exp Eye Res 1971; 12: 275-281.*
3. *Bill A. The drainage of albumin from the uvea. Exp Eye Res 1964; 75: 179-187.*
4. *Bill A. Conventional and uveo-scleral drainage of aqueous humor in the cynomolgus monkey (Macaca irus) at normal and high intraocular pressures. Exp Eye Res 1966; 5: 45-54.*
5. *Gasterland D, Kupfer C. Experimental glaucoma in the rhesus monkey. Invest Ophthalmol 1974; 13: 455-457.*
6. *Krupin T, Kolker AE, Kass MA, Becker B. Intraocular pressure the day of argon laser trabeculoplasty in primary open-angle glaucoma. Ophthalmology 1984; 91: 361-365.*
7. *Shingleton BJ, Richter CU, Bellows AR, Hutchinson BT, Glynn RJ. Long-term efficacy of argon laser trabeculoplasty. Ophthalmology 1987; 94: 1513-1518.*
8. *Thomas JV, Simmons RJ, Belcher CD 3rd. Argon laser trabeculoplasty in the presurgical glaucoma patient. Ophthalmology 1982; 89: 187-197.*
9. *Simon G. Vivar A, Lowery JA. Clinical results following gonioscopic laser trabecular ablation (GLTA) with a Ti:Sapphire laser for the treatment of glaucoma. Invest Opthalmol Vis Sci 1995; 36: S838. Abstract No 3861.*
10. *Manns F, Parel JM, Fernandez V, Stoiber J, Lamar P, Salas N, et al. Qualitative-optical thermal model of argon, selective, and microsencond infrared laser trabeculoplasty. Opthalmic Technologies XIII 2003; 4951: 71-76.*
11. *Parel JM, Ren Q, Simon G. Noncontact laser photothermal keratoplasty. I: Biophysical principles and laser beam delivery system. J Refract Corneal Surg 1994; 10: 511-518.*
12. *Alexander RA, Grierson I. Morphological effects of argon laser trabeculoplasty upon the glaucomatous human meshwork. Eye 1989; 3: 719-726.*
13. *McMillan TA, Stewart WC, Legler UF, Powers T, Nutaitis MJ, Apple DJ. Comparison of diode and argon laser trabeculoplasty in cadaver eyes. Invest Ophthalmol Vis Sci 1994; 35: 706-710.*
14. *Kramer TR, Noecker RJ. Comparison of the morphologic changes after selective laser trabeculoplasty and argon laser trabeculoplasty in human eye bank eyes. Ophtalmology 2001; 108: 773-779.*
15. *Wise JB, Witter SL. Argon laser therapy for open-angle glaucoma. A pilot study. Arch Ophthalmol 1979; 97: 319-322.*
16. *Wise JB. Errors in laser spot size in laser trabeculoplasty. Ophthalmology 1984; 91: 186-190.*
17. *Starita RJ, Fellman RL, Spaeth GL, Poryzees E. The effect of repeating full-circumference argon laser trabeculoplasty. Ophthalmic Surg 1984; 15: 41-43.*
18. *Brown SV, Thomas JV, Simmons RJ. Laser trabeculoplasty re-treatment. Am J Ophthalmol 1985, 99: 8-10.*
19. *Stoiber J, Fernandez V, Lamar PD, Decker SJ, Dubovy S, Hitzl W, et al. Trabecular meshwork alteration and intraocular pressure change following pulsed near-infrared laser trabeculoplasty in cats. Ophthalmic Surg Lasers Imaging 2005; 36: 471-481.*